24th COBEM - 2017

24th ABCM International Congress of Mechanical Engineering
December 3-8, 2017, Curitiba, PR, Brazil

COBEM-2017-1602
THE BACKSCATTER ON LARGE EDDY SIMULATION AND ON SOLUTION OBTAINED WITH NON-LINEAR DISTURBANCE EQUATION.

Ricardo Galdino da Silva
E-mails: $ri\_galdino@yahoo.com.br$
Marcos de Mattos Pimenta
E-mails: $marcos.pimenta@poli.usp.br$
Escola Politénica da USP - Av. Prof Luciano Gualberto, Travessa 3 n 380, Butantã, São Paulo, 05508-010, Brasil

Abstract. *We apply a Large Eddy Simulation with subgrid stress computed by means of an additional transport equation for subgrid kinetic energy and an approach to solving turbulence flow based on Non-Linear Disturbance Equation to solve fully developed turbulent channel flow at $Re_\tau = 395$. The open source code, called OpenFOAM, is used in the present effort. From the numerical results, firstly, the backscatter, which is the energy transfer in inverse direction of a Richardson cascade of energy (the energy is transfer from big scale to the small scale), is quantified. Secondly, the mesh refinement effect on the backscatter and on the accuracy of the solution is analyzed for Large Eddy Simulation and Non-Linear Disturbance Equation. Finally, we correlate the solution accuracy with the lack or excess of backscatter and forward-scatter. The solutions obtained with the most refined mesh and Non-Linear Disturbance Equation show that the maximum effect of backscatter takes place in buffer-layer of channel boundary layer. In addition, the solutions computed with Non-Linear Disturbance Equation present more turbulent fluid dynamics, which can be measured by turbulent energy dissipation associated with backscatter and forward-scatter, than those obtained with Large Eddies Simulations.*

Keywords: *CFD, Turbulence Model, Backscatter, Large Eddy Simulation, Turbulent Channel Flow*

1. INTRODUCTION

The flow over a aircraft in its land configuration (high-lift surfaces deployed) is a complex simulation, not only due to a complex geometry but also because of the complexity of flow its, which consist in interactions between vortex, a confluence of boundaries layers and wakes, flow separations due to adverse pressure gradients, etc.... The Brazilian aircraft industry usually uses a Reynold Averaged Turbulence model (RANS) approach to simulate such a complex flows. However, this approach could be out of its range of applicability, since the physical phenomena present in such flow, mostly for flow at configurations near the aircraft stall (maximum lift), is not accurately resolved by Reynold Averaged Navier-Stokes Turbulence model. In order to deal with flow features present in such flow, more physical features of turbulence must be resolved instead of modeling. This task is done by turbulence model in which part of turbulence scales are solved and the rest of turbulence scales is modeled (Large Eddy Simulations - LES), or even solve the whole turbulence scales (Direct Navier-Stokes - DNS). For Reynolds Averaged Navier-Stokes Turbulence models, the whole turbulence scales are modeled.

The Large Eddy Simulation models are time-consuming and also need a high computational power, since the simulation is time accurate and require a fine mesh. In other words, it means that these methodologies are much more expensive than Reynolds Averaged Navier-Stokes and use this kind of simulation in the design process of high-lift devices, for instance, is thus prohibitive nowadays. Moreover, all subgrid model based Smagorinsky subgrid model (Smagorinsky, 1963) introduce a dissipation, which means a drainage of turbulent energy transported from large scale to small scale (Richardson energy cascade, forward-scatter). However, Piomelli *et al.* (1990) observed that the transfer of energy from small scale to big scale (backscatter; energy transfer in inverse direction of Richardson cascade) affects the instabilities growth in the laminar to the turbulent transition process. In addition, Piomelli *et al.* (1991) pointed out that in a Directed Numeric Simulation of channel flows the fifth percent of mesh cell present backscatter. The presence of backscatter does not contradict Richardson's concepts of energy cascade, once in the average, the turbulence energy transfer is still from bigger scales to small scales (Mason and Thomson, 1992) and the dissipation should only decrease. In addition, it effects is still draining the energy. Another drawback of Large Eddy Simulation is excessive mesh refinement needed to be able to predict the near-wall effects. The dynamic model proposed by Germano *et al.* (1991) and Lilly (1992) tend to generate

a negative eddy viscosity (related to subgrid stress tensor), which is the related to the backscatter. However, it is normally avoided since it leads to numerical instability. The requirements need to one be able to use Direct Numerical Simulation (DNS) is tighter than for Large Eddy Simulation, and it is used just for simple problems, such as channel flow at low Reynolds number. Therefore, those approaches are not common in an industrial process.

This article reports part of the process to achieve a bigger objective, which is developing a numerical methodology that is able to the predict a turbulence flow with the same resolution capability of turbulent structures due to Large Eddy Simulation models, and also be able to deal with flow regions in the proximity of solid walls. This last requirement is a severe requirement for Large Eddy Simulation (LES) models since it has a dependency on the mesh refinement in these regions. Both requirements of this new methodology should be achieved with less mesh refinement than a Large Eddy Simulation requires. The new turbulence methodology approach is based on Non-Linear Disturbance Equation (NLDE), that is normally used to acoustics simulation and it was first proposed by Morris *et al.* (1997) and extended by Batten *et al.* (2004) in conjugation with a Synthesized Turbulence Method developed by (Billson, 2004) in order to introduce the backscatter that comes from the subgrid flow structures, structures that the mesh has not enough resolution to deal with. In the present effort, we use only the NLDE, in other words, it is not considered the backscatter that comes from the subgrid flow structures. Since our main go is to predict the backscatter and relate that with flow simulation results.

The test case to be used in this article is the full turbulent channel flow at $Re_\tau = 395$. This case was simulated by Moser *et al.* (1999) and Kim *et al.* (1987) by means of a Direct Numerical Simulation (DNS). All the numerical results obtained in this effort will be compared to the Moser *et al.* (1999) and Kim *et al.* (1987) results, which are considered as a reference in our comparisons. The backscatter and forward-scatter will be quantified for each combination of turbulence model and mesh refinement levels. The lack or even the excess of these transfer energy phenomenon will be related to the accuracy of numerical results.

2. THEORETICAL AND NUMERICAL FORMULATION

In this section, at first, the equation that governs the flow is shown (subsection 2.1). After that, we will present a description of the turbulence models used in the present effort. These turbulence model consist of two model which were already available in OpenFOAM (subsection 2.2and 2.3) and a new proposal will be presented in the subsection 2.4 . A methodology to quantify the backscatter and the forward scatter will be exhibited in subsection 2.5 Finally, a brief description of numerical formulation used by OpenFOAM to solve flow will be given in subsection 2.6

2.1 Navier-Stokes Equations

Considering an incompressible flow, the conservation of mass and momentum equation takes the form:

$$\nabla \cdot u = 0 \tag{1}$$

$$\frac{\partial u}{\partial t} + \nabla \cdot (uu) = -\frac{1}{\rho}\nabla p + \nabla \cdot \left[\nu \left(\nabla u + \nabla u^T\right)\right] \tag{2}$$

in which u is the velocity field, p is the static pressure, ρ is the density and ν is the kinematic viscosity.

2.2 Reynold Averaged Navier-Stokes - RANS

The Reynolds Averaged Navier-Stokes equations is derived by means of an averaging process of the Navier-Stokes equations (Eq. 1 and Eq. 2). The mean flow field is defined by the ensemble average, which is given for a generic variable as:

$$\overline{V} = \frac{1}{N}\sum_{i=1}^{N} V_k \tag{3}$$

With this averaging operator, it is possible to split the flow fields between a mean value plus a fluctuation, which orbits around the mean value and also have its mean value equal to zero. This decomposition is known as Reynolds decomposition. Thus the flow field takes the following form:

$$V = \overline{V} + V' \tag{4}$$

In order to obtain the Reynolds-averaged Navier-Stokes, first, we replace the variable of Navier-Stokes equation for its decomposition (defined by Eq. 4) into the Navier-Stokes equations and then we apply the mean operator defined by

Eq. 3 to this new equation. These steps are known as Reynolds averaging process. For an incompressible flow, the Navier-Stokes equations in its mean form or Reynolds Averaged form are:

$$\nabla \cdot \overline{u} = 0 \tag{5}$$

$$\frac{\partial \rho \overline{u}}{\partial t} + \nabla \cdot \left(\rho \overline{uu} + \rho \overline{u'u'}\right) = -\nabla \overline{p} + \nabla \cdot \left[\mu \left(\nabla \overline{u} + \nabla \overline{u}^T\right)\right] \tag{6}$$

As a consequence of Reynolds averaging process, a new tensor appears in Eq. 7, that is known as Reynolds stress tensor and it must be modeled in order to close equation system given by Eqs. 5 and 7 and also overcome the turbulence closure problem. In 1877, Boussinesq introduced the eddy-viscosity concept (Wilcox, 1993), in which the Reynolds stress tensor is treated like the viscous stress tensor. The eddy-viscosity concept has been used for several turbulence models available in the literature. The Reynolds stress tensor obtained by means of Boussinesq eddy-viscosity hypothesis for incompressible flow takes the form of:

$$-\rho \overline{u'u'} = \mu_t \left(\nabla \overline{u} + \nabla \overline{u}^T\right) - \frac{2}{3} kI \tag{7}$$

The term $\nabla \overline{u} + \nabla \overline{u}^T$ can be rewriten as $\nabla \overline{u} + \nabla \overline{u}^T = \overline{S}$, in which $\overline{S}$ is the mean strain tensor. The term k is kinetic turbulent energy and it is equal to $k = \frac{1}{2}\sum_{i=1}^{3} \overline{u_i' u_i'}$. The last left hand term of equation is introduced to make the Reynolds stress tensor trace equal to twice of the kinetic turbulent energy. It is worth to mention that this last term is omitted for the Spalart-Allmaras turbulence model proposed by Spalart and Allmaras (1992) and Spalart and Allmaras (1994). We choose this turbulence model to be used in this article. The Spalart-Allmaras turbulence model is one equation model, in which a transport equation is derived for modified eddy viscosity ($\widetilde{\nu_t}$). The transport equation for modified eddy viscosity is:

$$\frac{\partial \widetilde{\nu_t}}{\partial t} + \nabla \cdot (\overline{u} \widetilde{\nu_t}) = C_{b1} \left(1 - f_{t2}\right) \overline{S} \widetilde{\nu_t} - \left[C_{w1} - \frac{C_{b1}}{\kappa^2} f_{t2}\right] \left(\frac{\widetilde{\nu_t}}{d}\right)^2 + \frac{1}{\sigma} \left[\nabla \cdot \left(\left(\nu + \widetilde{\nu_t}\right) \nabla \widetilde{\nu_t}\right) + C_{b2} \nabla \widetilde{\nu_t} \cdot \nabla \widetilde{\nu_t}\right] \tag{8}$$

The turbulent eddy viscosity is computed from:

$$\mu_t = \rho \widetilde{\nu_t} f_{v1} \tag{9}$$

$$\chi = \frac{\widetilde{\nu_t}}{\nu} \tag{10}$$

the term $\nu = \frac{\mu}{\rho}$ is the molecular kinematic viscosity.

2.3 Large Eddy Simulation - LES

The Large Eddy Simulations turbulence model was first proposed by Smagorinsky (1963), in which was assumed that small eddy movement was uniform and its main function was to carry the turbulence energy through the energy cascade process. These ideas created the expectation that it is possible to determine the effects of these small eddies on the flow. Furthermore, they make a flow division in a large and small eddy, those eddies are always associated with length scales. Usually, in a Large Eddy Simulations the large eddies, which contain most part of the turbulent energy, are solved during the simulation, once the boundary conditions affect those eddies. While, the small eddies, which by assumption exhibit a universal behavior, are modulated using semi-empiric models. In other words, the large eddies behavior are affected by flow characteristics and extract energy from the mean flow, whereas the small eddies behavior are independent of flow characteristics and transfer energy to smaller eddies.

The Large Eddy Simulation provides a means to compute the large eddies (specific eddy scales range) by a statical filtering process (spatial averaging). The filtering process is done by a convolution between a Navier-Stokes equation and the filter function (Gaussian filter, top-hat filter, Fourier filter, etc.). As result of this process, the spatial averaged Navier-Stokes equation is obtained.

Any flow variable, V, can be rewritten as a sum of its large scale contributions,$\tilde{V}$ and its small-scale contributions, $V^{''}$. Formally, it is given by:

$$V = \tilde{V} + V^{''} \tag{11}$$

After applying the filtering process to Navier-Stokes equations (Eq. 1 and Eq. 2) and considering the definitions given by Eq. 11, it is possible to obtain the spatial averaged Navier-Stokes equations. For an incompressible flow, they are given by:

$$\nabla \cdot \widetilde{u} = 0 \tag{12}$$

$$\frac{\partial \widetilde{u}}{\partial t} + \nabla \cdot (\widetilde{u}\widetilde{u}) = -\frac{1}{\rho}\nabla \widetilde{p} + \nabla \cdot \left[\nu \left(\nabla \widetilde{u} + \nabla \widetilde{u}^{T}\right)\right] - \nabla \cdot \tau_{sgs} \tag{13}$$

The term $\widetilde{p}$ is the filtered pressure and the term $\tau_{sgs} = \widetilde{uu} - \widetilde{u}\widetilde{u}$ is the stress tensor that appears as result of the filtering process (similar to Reynolds stress tensor in the Reynolds Averaged Navier-Stokes equations Eqs. 5 and 7). This term is known as subgrid stress tensor and tends to zero as the Δ also tends to zero. By the away, Δ is the filter width, which is proportional to the smallest scale wavelength kept by the filtering process.

The subgrid stress model should drain the energy from eddies scales bigger than the filter width (Δ). This behavior can be accomplished with an eddy-viscosity model. Therefore, the subgrid tensor is given by:

$$\tau_{sgs} = -\nu_{sgs}\widetilde{S} + \frac{2}{3}k^{''}I \tag{14}$$

in which the term ν_{sgs} is subgrid scale eddy-viscosity, the term $\tilde{S} = \frac{\left(\nabla \tilde{u} + \nabla \tilde{u}^{T}\right)}{2}$ is the filtered strain rate, and the term $k^{''}$ is the subgrid scale turbulent kinetic energy.

In addition to the eddy-viscosity concept, a transport equation for subgrid-scale turbulent kinetic energy is used in order to solve subgrid viscosity. This equation can be found by first subtracting the filtered momentum equation (Eq. 13) from its unfiltered version to obtain an equation for the subgrid-scale velocity field, $u^{''}$. This result is multiplied by subgrid scale velocity field and finally contracting this new equation gives as the transport equation for subgrid-scale turbulent kinetic energy, which is given by Yoshizawa (1985) apud Villiers (2006) as:

$$\frac{\partial \widetilde{u}}{\partial t} + \nabla \cdot \left(k^{''}\tilde{u}\right) = \nabla \cdot \left[\left(\nu + \nu_{sgs}\right)\nabla k^{''}\right] - \epsilon - \tau_{sgs} : \tilde{S} \tag{15}$$

the eddy-viscosity, ν_{sgs}, and the dissipation, ϵ, are defined as:

$$\nu_{sgs} = C_k \left(k^{''}\right)^{1/2} \Delta \tag{16}$$

$$\epsilon = \frac{C_\epsilon \left(k^{''}\right)^{3/2}}{\Delta} \tag{17}$$

2.4 Non-linear Disturbance Equation - NLDE

The velocity field is decomposed into a summation of a mean flow ($\bar{u}$), resolved fluctuation ($\breve{u}$) and a subgrid-scale fluctuation ($\hat{u}$). The term $\bar{u}$ is obtained by means of a Reynolds averaging process. The term $\breve{u}$ is the velocity field that the set of numerical method and mesh resolution is able to support, resolved part of velocity fluctuation. Finally, the term $\hat{u}$ is the part of the velocity field that set of numerical method and mesh resolution is not able to support, unresolved part or subgrid part of velocity fluctuation. The velocity decomposition takes the form of:

$$u = \overline{u} + \breve{u} + \widehat{u} \tag{18}$$

If the decomposition of velocity field given by Eq. 18 is substituted into the Navier-Stokes equations (Eq. 1 and Eq. 2). Thus, this process gives us the following equation:

$$\nabla \cdot (\overline{u} + \breve{u} + \widehat{u}) = 0 \tag{19}$$

$$\begin{aligned}&\frac{\partial\overline{u}}{\partial t}+\nabla\cdot(\bar{u}\bar{u})+\frac{\partial\breve{u}}{\partial t}+\nabla\cdot(\breve{u}\breve{u})+\frac{\partial\hat{u}}{\partial t}+\nabla\cdot(\hat{u}\hat{u})\\&+\nabla\cdot(\bar{u}\breve{u})+\nabla\cdot(\bar{u}\hat{u})+\nabla\cdot(\breve{u}\bar{u})+\nabla\cdot(\breve{u}\hat{u})+\nabla\cdot(\hat{u}\bar{u})+\nabla\cdot(\hat{u}\breve{u})\\&=\tfrac{1}{\rho}\left[-\nabla p+\mu\nabla^2\left(\bar{u}+\breve{u}+\hat{u}\right)\right]\end{aligned}\tag{20}$$

Finally, we use the Reynolds Averaged Navier-stokes equations to simplify the Eq. 5 and 7. These simplifications drive as to find the Non-Linear Disturbance Equations, which are given by:

$$\nabla\cdot(\breve{u}+\widehat{u})=0\tag{21}$$

$$\begin{aligned}&\frac{\partial\breve{u}}{\partial t}+\nabla\cdot(\breve{u}\breve{u})+\frac{\partial\hat{u}}{\partial t}+\nabla\cdot(\hat{u}\hat{u})\\&+\nabla\cdot(\bar{u}\breve{u})+\nabla\cdot(\bar{u}\hat{u})+\nabla\cdot(\breve{u}\bar{u})+\nabla\cdot(\breve{u}\hat{u})+\nabla\cdot(\hat{u}\bar{u})+\nabla\cdot(\hat{u}\breve{u})\\&=\tfrac{1}{\rho}\left[-\nabla\grave{p}+\mu\nabla^2\left(\breve{u}+\hat{u}\right)\right]+\nabla\cdot\tau_t\end{aligned}\tag{22}$$

in which, $\grave{p}=p-\bar{p}$ is the difference between the instantaneous pressure field and averaged pressure field, and τ_t is the Reynolds stress tensor. The averaged velocity field ($\bar{u}$) and the Reynolds stress tensor (τ_t) came from a priori numerical simulation which uses, for instance, a Reynolds-averaged Navier-Stokes turbulence model. Thus, $\bar{u}$ and τ_t are both known Before we begin the resolution of the system given by Eq. 21 and Eq. 22. In our case, for the simulations that will be presented in section 3. these fields will came from DNS solution obtained by Kim *et al.* (1987) and Moser *et al.* (1999) and from a numerical solution using the Spalart-Allmaras (sub-section 2.2 gives the model description) turbulence model, which have been done by the authors.

Equation 21 and Eq. 22 also depend on which we call a subgrid velocity fluctuations field ($\hat{u}$). This unsteady fluctuation could be calculated using a methodology proposed by Billson (2004) to generate a synthesized turbulence field. However, for the present effort, this formulation will be left out and the ($\hat{u}$) will be considered to be equal to zero. Since, $\bar{u}$ and τ_t are known from a priori numerical simulation. The disturbance (fluctuation) will be determined as result of a numerical system given by Eqs. 21 and 22.

2.5 Backscatter

In order to quantify the energy transfer from resolved scales to unresolved scales (subgrid scales) and also the energy transfer from unresolved scale to resolved scale, which is related to forward-scatter events and backscatter events in the turbulent cascade process of energy transfer. A transport equation for filtered kinetic energy (kinetic energy based on the resolved velocity field),$\tilde{k}=\tilde{u}\cdot\tilde{u}$, takes the form:

$$\frac{\partial\tilde{k}/2}{\partial t}+\nabla\cdot\left(\tilde{u}\tilde{k}/2\right)=-\frac{1}{\rho}\nabla\cdot\tilde{u}\tilde{p}-\nabla\cdot(\tilde{u}\cdot\tau_{sgs})+\nu\nabla\cdot\nabla\tilde{k}/2-\nu\nabla\tilde{u}:\nabla\tilde{u}-\tau_{sgs}:\tilde{S}\tag{23}$$

The last term of Eq. 23 right-hand side ($\varepsilon_{sgs}=-\tau_{sgs}:\tilde{S}$) is the subgrid-scale dissipation. It is obtained from a contraction of subgrid-scale stress tensor (τ_{sgs}) and filtered strain rate tensor ($\tilde{S}$; strain rate calculated from the resolved or filtered velocity field). This dissipation term represents the energy transfer between resolved and unresolved scales (Piomelli *et al.*, 1991). In addition, it is a summation of several terms. When one of these terms is positive, the energy transfer occurs from large-scales to small-scale (forward-scatter - ε^+). On the other hand, when it is negative, the energy transfer takes place from small-scale to large-scale (backscatter - ε^-). Thus, subgrid-scale dissipation is the summation of terms that represent energy transfer in the direction of original energy cascade direction (forward-scatter) and terms that represent energy transfer in the opposite direction of original energy cascade direction. In the average, the dissipation term should represent a process in which the energy is transfer from large-scale eddies to small-scale eddies. In other words, the presence of the backscatter in the energy transfer process does not disagree with the Richardson's energy cascade concept. Since, the net balance of ε^+ and ε^- is a positive value, which is consistent with concept mentioned.

The backscatter contribution for the energy transfer process will account by means of summation of all negative terms, and the forward contribution by means of summation of positive terms. The terms of ε_{sgs} will be calculated by a filtering process similar to the process used to obtain the equations of Large Eddy Simulation model (sub-section 2.3). The subgrid-scale dissipation is given by:

$$\varepsilon_{sgs} = \varepsilon_{NET} = -\tau_{sgs} : \tilde{S} = -\left(\widetilde{uu} - \tilde{u}\tilde{u}\right) : \frac{\left(\nabla\tilde{u} + \nabla\tilde{u}^T\right)}{2} = \sum\left(\varepsilon^+ + \varepsilon^-\right) \tag{24}$$

The ε_{NET}, ε^+, ε^- are related to the filter length used on the equation filtering processes for a given flow field and also grid resolution. Those measure a local dissipation associated with the filter length, thus those bring information from the energy transfer processes of eddies with length scale bigger than the cell mesh characteristic length and smaller than filter length. In other words, it is an image of the forward-scatter and backscatter processes for eddy with scales that ranging from cell mesh characteristic length (local small-scale) to filter length (local large-scale).

2.6 Numerical Methodology

The numerical methodology used in OpenFOAM is the finite volume method (Villiers, 2006). The computational space is divided into control volumes, and the properties are calculated at their centroids. The flow proprieties are stored in a co-located way, which means that the speed and pressure are stored at the same point. In order to avoid problems due to co-location, for instance, field oscillation and problems for the evaluation of the pressure gradient in the volume faces, the Rhie-Chow interpolation proposed by Rhie and Chow (1983) apud Mangani (2008) are used. The coupling between the field of velocities and pressure is performed through the procedure PISO (Pressure-Implicit with Splitting of Operators) proposed by Issa *et al.* (1986). The process of time integration is performed through the Second Order Backward Differencing method. The algebraic system resulting from the application of temporal and spatial discretization is solved through an iterative Gauss-Seidel method. The gradients of flow properties are computed by means of the Green-Gauss theorem. The numerical methodology that has been summarized in a simplified way is applied for all turbulence models previously described. For further details on the discretization process, can be found in Villiers (2006).

3. RESULTS

The test case, as mentioned earlier, is the full turbulent channel flow at $Re_\tau = 395$. The simulation conducted by Moser *et al.* (1999) and Kim *et al.* (1987) by means of a Direct Numerical Simulation (DNS) will be used as reference values. In our case, the time step used in the unsteady simulation is equal to 0.01 s and the total time simulated to computed the averaged results are equal to 30 times the time that a fluid particle takes to go through the entire channel length, in which the assembled averaged is computed with 600 realizations of flow, the time step between each realization is equal to 3 seconds. The channel dimensions used in present effort is $2\mathrm{m}x2\mathrm{m}x4\mathrm{m}$. In addition, the boundaries conditions are periodic at inflow, outflow and the at sides of the channel and nonslip wall at channel walls.

The results shown in this section were obtained with turbulence methodologies described in section 2.3and 2.4in combination with two types of mesh refinement. The mesh type M1 is a mesh usually used in Reynolds Averaged Turbulence Model approach, in which the refinement is bigger near the wall and the element size is stretched to its maximum size at the canal center. On the other hand, the mesh type M2 is a regular mesh with cell size equal in the whole space. The numerical solutions present in this section is identified by three names separated by the underline symbol. The first one refers to the mesh type, as mentioned. The second one, for M1 mesh type, represents the distance from the first cell face to the solid wall, moreover, this cell face is located in opposite side of the wall. In addition, for M2 mesh type represents the $Y+$ based on characteristic length of mesh cells, which is constant for that type of mesh. The last one is related to the turbulence model used in the numerical solution (LES, NLDE and NLDE/RANS).

Figures 1(a) and 1(b) show the non-dimensional velocity profile and non-dimensional turbulent kinetic energy as a function of Y^+ for numerical simulations. The worse result for non-dimensional velocity profile is given by Large Eddy Simulation with mesh type M2. From Fig. 1(a) it is possible to The discrepancy between LES results and DNS results decreases when the near wall mesh refinement is increased. The results from mesh M1_10-2_LES presents the smaller discrepancy from DNS solution at the log-law layer region of the boundary layer when its discrepancy is compared with the discrepancy obtained from mesh M2_16_LES and from M1_10-4_LES. On the other hand, the result at the buffer-layer region is the worst of all three meshes. The results from M1_10-4_LES has smaller discrepancy at viscous sublayer ($Y^+ > 5$) and buffer-layer ($5 < Y^+ < 60$) of boundary layer. However, the result at log-law layer ($Y^+ > 60$) is worst than the result for a mesh with less refinement. The behavior is odd, it was expected that M1_10-4_LES result was better than M1_10-2_LES since the mesh refinement should improve the physical resolutions of numerical simulation and as a consequence, the discrepancy should decrease.

From 1(b) it is possible to observe that the position obtained with all Large Eddy Simulation simulation of maximum k^+ is found to be displaced in comparison to the position indicated by DNS simulation of Moser *et al.* (1999). The maximum value of k^+ improves with mesh refinement, from M1_10-4_LES to M1_10-2_LES. Moreover, the maximum value is overpredicted by the simulation with M2_16_LES. Not only could be all the discrepancies found in LES simulations a result of mesh refinement effect, but also an effect of the subgrid model (described in section 2.3)chosen for those simulations.

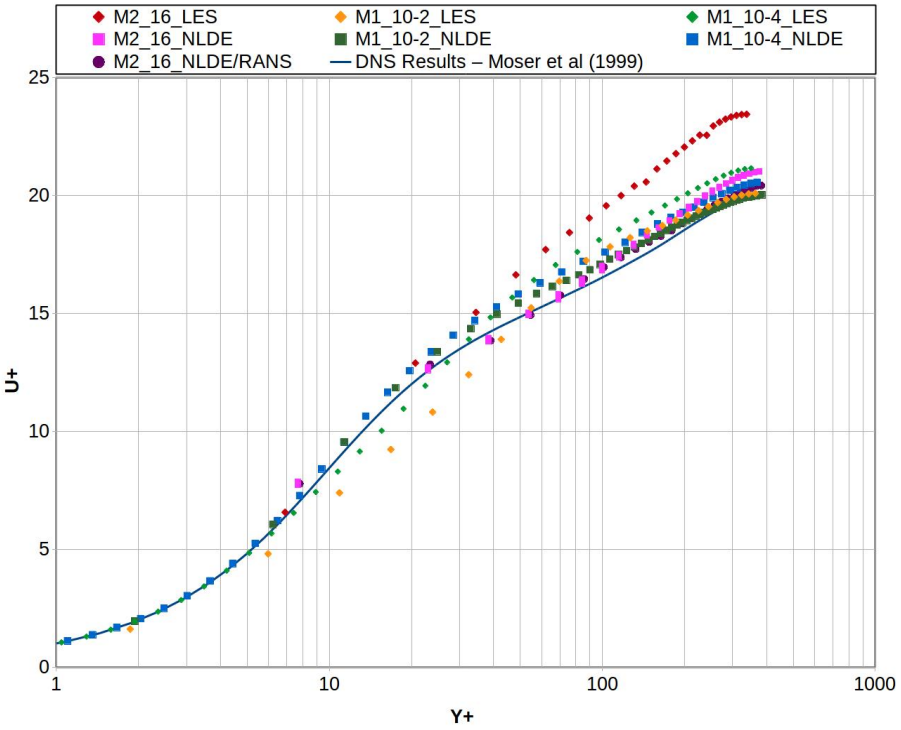

(a) Non-Dimensional Boundary layer velocity profile, in which $U^+ = \frac{\overline{U}}{U_\tau}$ and $Y^+ = \frac{\rho h U_\tau}{\nu}$.

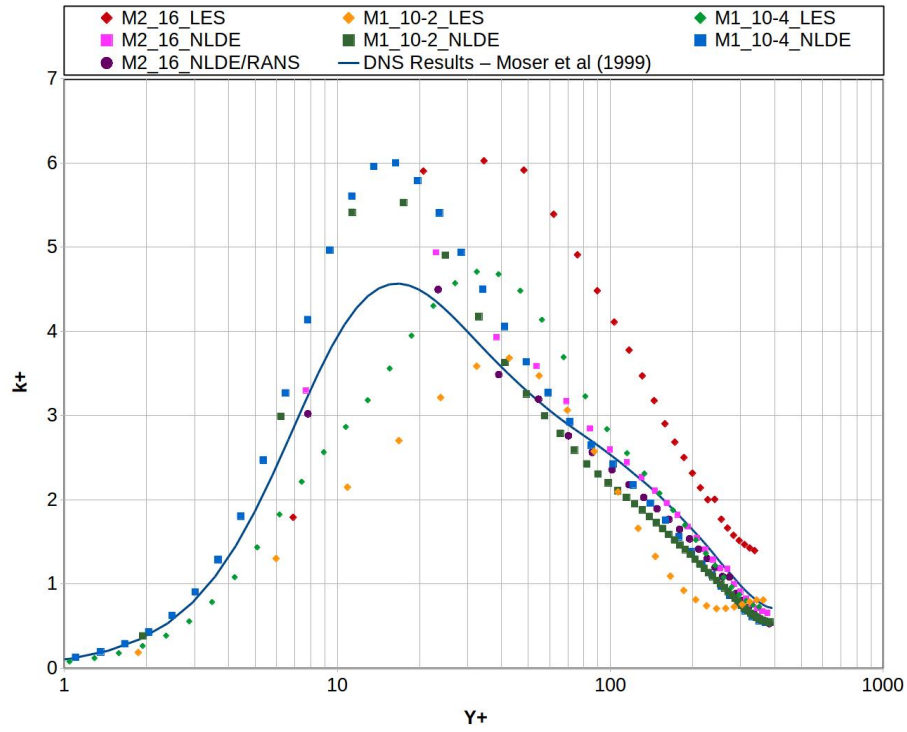

(b) Non-Dimensional Turbulent Kinetic Energy $k^+ = \frac{\frac{1}{2}\sum_{i=1}^{3}\overline{u_i' u_i'}}{U_\tau^2}$.

Figure 1. Non-dimensional profile of k^+ (kinetic turbulent energy) and U^+ (velocity) for simulations using LES turbulence model, NLDE turbulence model (the averaged properties needs in such model (Eq. 21 and Eq. 22) is obtained by means of interpolating the DNS results (Moser *et al.*, 1999) on each mesh) and NLDE/RANS turbulence model (the averaged properties need to solve Eq. 21 and Eq. 22 comes from a stead simulations with SA turbulence model). The best results is the one obtained with NLDE/RANS turbulence model for both profile k^+ and U^+.

The results of U^+ improve for the all NLDE (M2_16_NLDE, M1_10-2_NLDE and M1_10-4_NLDE) simulation when it is compared to LES results. Also, the k^+ maximum position is better predicted with methodologies that use a Non-Linear Disturbance Equation (NLDE). However, the value of maximum k^+ is overpredicted by all results obtained with this turbulence model. It is worth to mention that, all the averaged values needed to solve the system of equations formed by Eqs. 21 and 22 are interpolated from the averages obtained from DNS results (Moser *et al.*, 1999).

The NLDE\RANS turbulence model improves not only the prediction of the velocity profile but also the result of turbulent kinetic energy, k. Those results are presented in Fig. 1(a) and Fig. 1(b) with the name M2_16_NLDE\RANS. The results became better than the other simulation in all regions of the boundary layer and the same is observed for turbulent kinetic energy, k, values.In the beginning, it was expected that the NLDE (with DNS) results would be similar or even better than those obtained with RANS. Since the average values are obtained with DNS results. The justification for the discrepancies found [and attributed to the interpolation process used to transfer the DNS results to our mesh.

Figures 2(c), 2(a) and 2(b) show the dissipation terms calculated with the methodology explained in section 2.5, in which it uses the filtering process of resolved field obtained by Large Eddy Simulation with three meshes. Those mesh has a different global refinement and also near wall refinement. The curves in those figures should not be directed compared, once these are related to the effects of different scales (size of the characteristic length of the filter are different for each mesh). Anyway, all simulations exhibit the presence energy transfer in both directions, forward-scatter (Fig. 2(a)) and backscatter (Fig. 2(b)). The net balance between these energy transfer direction is positive for all boundary layer regions (log-law layer, the buffer layer, and viscous sublayer) for simulation with M1 mesh type (mesh with a near wall refinement; the cell that a close to the wall has with a large aspect ratio). On the other hand, the net balance results obtained with M2 mesh type oscillate between positive and negative value. It is worth to mention that the effect related to the Large Eddy Simulation subgrid model was not included in the results presented in Fig. 2. This contribution should be positive, once it takes into account only the forward-scatter. Because of that, the forward-scatter should increase if we include the subgrid effect.

A comparison between results obtained with Large Eddy Simulation and Non-Linear Disturbance equation results are presented in Fig. 3. The net balance, forward-scatter, and backscatter are shown in Figs. 3(c), 3(a) and 3(b) respectively. The forward-scatter and backscatter increase significantly for all meshes used in these simulations. The levels of dissipation introduced by the forward and backward process of energy transfer are similar. However, the net balance goes from positive (forward-scatter) to negative (backscatter) due to a mesh refinement effect. It becomes negative in all regions of the channel boundary layer for results obtained with M2 mesh type, which is an indication that backscatter dominates in all domain. This result seems odd since on the average we should obtain positive balance result, as the consequence the average of turbulence energy transfer process was given in the direction of the larger scales to the smaller scales. For the M2_16_NLDE and M2_16_NLDE\RANS type, the Richardson's energy cascade concept is not valid, at the list for spatial filter width equal to double of the cubic root of the cell volume. On the other hand, the results of M1_10-4_NLDE agree with the Richardson's concept. In addition, the results of M1_10-2_NLDE agree with this concept for cells with Y^+ greater than 10 and is not respected for Y^+ smaller than 10. The peak of forward-scatter and backscatter take places on the buffer-layer region for all results obtained with NLDE.

From the comparisons shown in Figs. 3(a), 3(b) and 3(c), it possible to observe that the numerical simulations done with LES turbulence model present a lack of turbulent fluid dynamics in the scale range from cell mesh size and the filter length. This could be associated with an excess of dissipation introduced by subgrid model. This conclusion was found by means of the comparisons done between LES and NLDE results. In addition, the NLDE solutions and NLDE/RANS solution present a more turbulent fluid dynamics, at least, in the considered scale range. The turbulent fluid dynamics of each turbulence model was measured by considering the amount of dissipation generated by forward-scatter and backscatter. Since these are a measure of the interaction between fluctuations of the turbulent velocity field, which are directly associated with the turbulent fluid dynamics of the flow. It is worth to mention that the comparison of the forward-scatter and backscatter should be made just for groups of the solution obtained with the same mesh. Comparison between different mesh is not appropriated because forward-scatter and backscatter are computed considering different ranges of length scale.

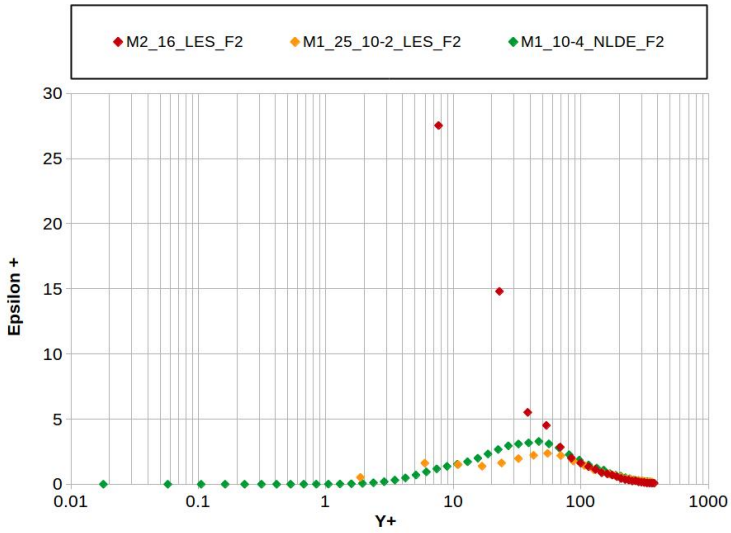

(a) Forward-scatter.

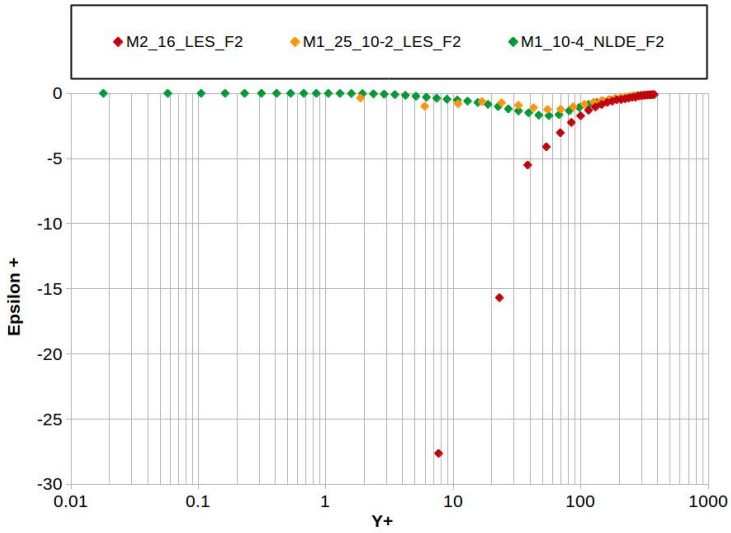

(b) Backscatter.

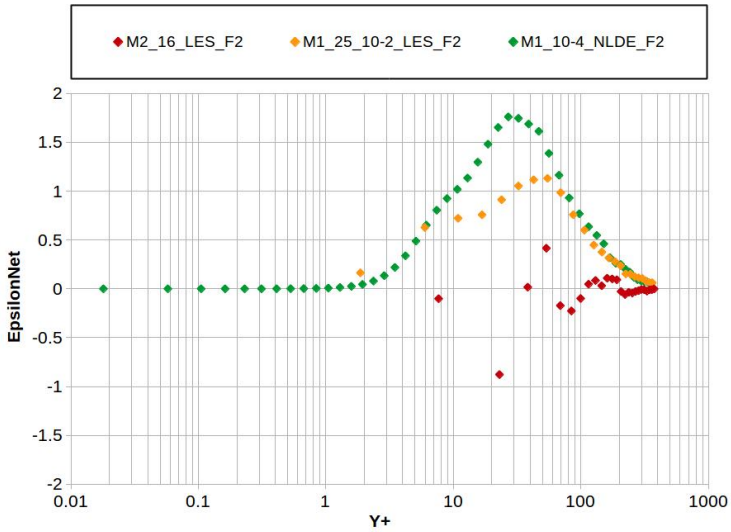

(c) Net balance between forward-scatter and backscatter.

Figure 2. Dissipation terms (forward-scatter and backscatter) of kinetic energy equation (Eq. 23). They are calculated through a spatial filtering process of the resolved velocity field and its gradient.The characteristic length used in filtering process and it means that the characteristic length is equal to twice the cubic root of local mesh cell volume (F2).

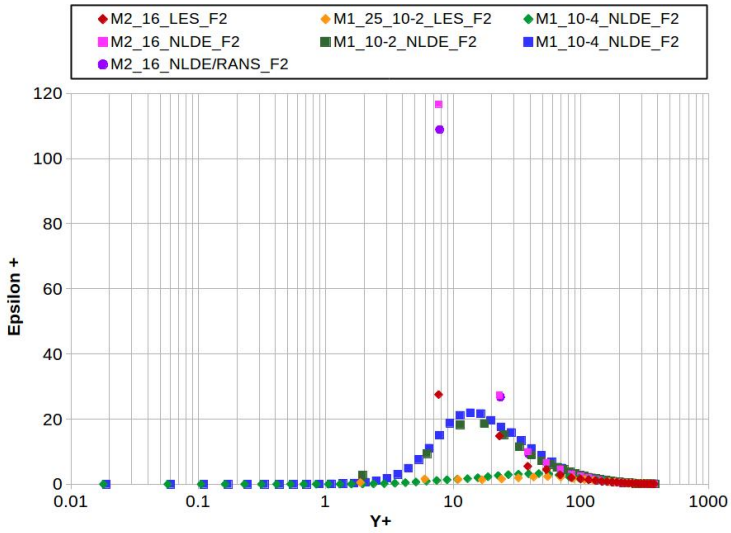

(a) Forward-scatter.

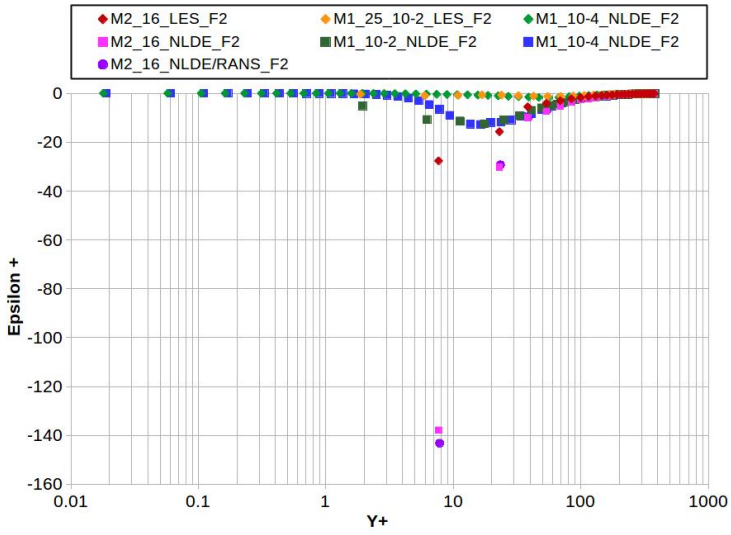

(b) Backscatter.

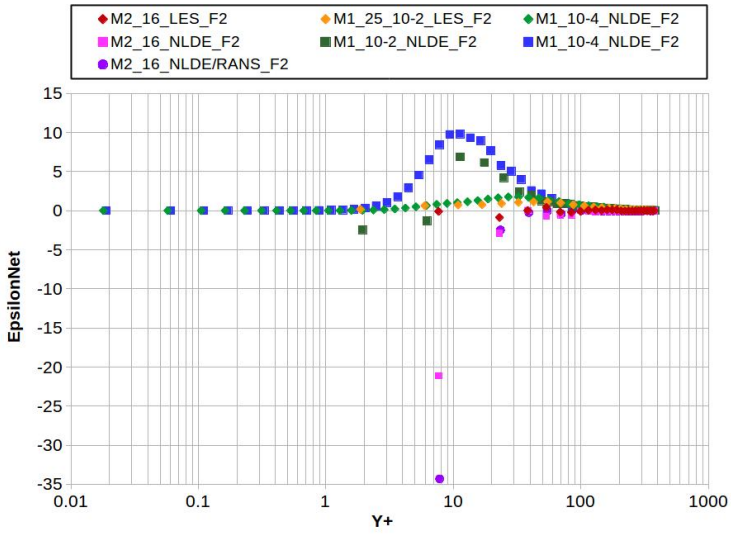

(c) Net balance between forward-scatter and backscatter.

Figure 3. Dissipation terms (forward-scatter and backscatter) of kinetic energy equation (Eq. 23). They are calculated through a spatial filtering process of velocity field ($u = \overline{u} + \breve{u} + \widehat{u}$) and its gradient.The characteristic length used in filtering process and it means that the characteristic length is equal to twice the cubic root of local mesh cell volume (F2).

4. CONCLUDING REMARKS

The solutions obtained with all mesh NLDE turbulence model in the present effort show that the maximum turbulent kinetic energy transfer by means of backscatter process take place in buffer-layer of channel boundary layer. The same behavior is observed for the forward-scatter process. Furthermore, the pick of turbulent kinetic energy, k, occurs also inside the buffer layer, the results obtained with NLDE/RANS turbulence model present the best matching with DNS results. All other NLDE results overpredict the maximum k. On the hand, the position of the k pick is shifted for all results obtained with LES turbulence model when those are compared to DNS.

The solutions obtained with LES turbulence model seems to have an excess of dissipation, probably introduces by their subgrid models. As consequence, the turbulent fluid dynamics is decreased, which is directed linked to the interaction between vortex from different scales. These declining on interactions affect directly the forward-scatter and backscatter. From the observation that has been made so far, this possible lack of forward-scatter and backscatter are the cause of discrepancies observed between solutions obtained with LES turbulence model and NLDE turbulence model.

We would like to emphasize that all results obtained with NLDE turbulence model, even in meshes without special refinement in the near wall region, presents better match with DNS results than those obtained with LES turbulence models. The NLDE for all meshes, with DNS and RANS, present a backward and forward-scatter much greater than those computed for solutions obtained with LES turbulence model. This observation is an evidence that solutions obtained with NLDE present more turbulent fluid dynamics when they are compared with the LES turbulence model results. In other words, it is an evidence that NLDE turbulence model is less dissipative than LES turbulence model, at least, for the subgrid model used in the present effort. Finally, the backscatter becomes dominant, which means a negative net balance between turbulent energy transfer related with backscatter and forward-scatter, when the mesh refinement is decreased. For the coarsest mesh, the backscatter is dominant in all regions of the boundary layer.

5. REFERENCES

Batten, P., Ribaldone, E., Casella, M. and Chakravarthy., S., 2004. "Towards a generalized non-linear acoustics solver." In AIAA, ed., *10th AIAA/CEAS Aeroacoustics Conference*. AIAA 2004-3001.

Billson, M., 2004. *Computational Techniques for Turbulence Generated Noise*. Doktorsavhandlingar vid Chalmers tekniska hÃűgskola. Ny serie, no: 2105. Department of Thermo and Fluid Dynamics, Chalmers University of Technology,. ISBN 91-7291-423-8.

Germano, M., Piomelli, U., Moin, P. and Cabot, W.H., 1991. "A dynamic subgridscale eddy viscosity model." *Phys. Fluids A*, Vol. 3, pp. 1760–1765.

Issa, R.I., Gosman, A.D. and Watkins, A.P., 1986. "The computation of compressible and incompressible recirculating flow by a non-iterative implicit scheme." *Journal of Computational Physicsl*, Vol. 62, pp. 66–82.

Kim, J., Moin, P. and Moser, R., 1987. "Turbulence statistics in fully developed channel flow at low reynolds number". *J. Fluid Mech*, Vol. 177, pp. 133–166.

Lilly, D.K., 1992. "A proposed modification of the germano subgridscale closure method." *Phys. Fluids A*, Vol. 4, pp. 633–635.

Mangani, L., 2008. *Development and Validation of an Object Oriented CFD Solver for Heat Transfer and Combustion Modeling in Turbomachinery Applications*. Ph.D. thesis, UniversitÃă degli Studi di Firenze, FacoltÃă di Ingegneria, Dipartimento di Energetica âĂIJSergio Stecco.

Mason, P.J. and Thomson, D.J., 1992. "Stochastic backscatter in large-eddy simulations of boundary layers". *J . Fluid Mech.*, Vol. 242, pp. 51–78.

Morris, P.J., Long, L.N., Bangalore, A. and Wang., Q., 1997. "A parallel three-dimensional computational aeroacoustics method using nonlinear disturbance equations." *J. Comput. Phys,*, Vol. 133, pp. 56–74.

Moser, R.D., Kim, J. and Mansour, N.N., 1999. "Airect numerical simulation of turbulent channel flow up to reÏĎ = 590." *Physics of Fluids*, Vol. 11, No. 4, pp. 943–945.

Piomelli, U., Cabot, W.H., Moin, P. and Lee, S., 1991. "Sub-grid scale backscatter in turbulent and transitional flows." *Phys. of Fluids A*, Vol. 3, pp. 1766–1771.

Piomelli, U., Zang, T.A., Speziale, C.G. and Hussaini, M.Y., 1990. "On the large eddy simulation of transitional wall bounded flows." *Phys. of Fluids A*, Vol. 2, pp. 257–265.

Rhie, C.M. and Chow, W.L., 1983. "Numerical study of the turbulent flow past an airfoil with trailing edge separation." *AIAA Journal*, Vol. 21, pp. 1525–1532.

Smagorinsky, J., 1963. "General circulation experiments with the primitive equations i. the basic experiment." *Monthly Weather Review*, Vol. 91, No. 8, pp. 99–164.

Spalart, P.R. and Allmaras, S., 1992. "A one-equation turbulence model for aerodynamic flows". *30th Aerospace Sciences Meeting and Exhibit,Aerospace Sciences Meetings, American Institute of Aeronautics and Astronautics*.

Spalart, P.R. and Allmaras, S., 1994. "A one-equation turbulence model for aerodynamic flow." *La Recherche Aeropastiale*, Vol. 1, pp. 5–21.

Villiers, E., 2006. *The Potential of Large Eddy Simulation for the Modeling of Wall Bounded Flows*. Ph.D. thesis, Imperial College of Science, Technology and Medicine.

Wilcox, D.C., 1993. *Turbulence modelling for CFD*. DCW Industries, La Cañada, 3rd edition.

Yoshizawa, A., 1985. "A statistically-derived subgrid-scale kinetic energy model for the large-eddy simulation of turbulent flows." *Journal of the Physical Society of Japan*, Vol. 54, No. 8, pp. 2834–239.

6. RESPONSIBILITY NOTICE

The authors are the only responsible for the printed material included in this paper.